Mapping the Reversible Charge State Control of an Iron Tetraphenyl Porphyrin Molecule Adsorbed on a CaF 2 /Si(100) Semi-Insulating Surface at Low Temperature (9 K)

Eric Duverger, Damien Riedel

Mapping the Reversible Charge State Control of an Iron Tetraphenyl Porphyrin Molecule Adsorbed on a CaF2/Si(100) Semi-insulating Surface at Low Temperature (9 K)

Journal:	*The Journal of Physical Chemistry*
Manuscript ID	jp-2024-02455a.R1
Manuscript Type:	Article
Date Submitted by the Author:	20-Jun-2024
Complete List of Authors:	Duverger, Eric; FEMTO-ST, Université de Franche Comté Riedel, Damien; CNRS, Institut des Sciences Moléculaire d'Orsay

TOC file

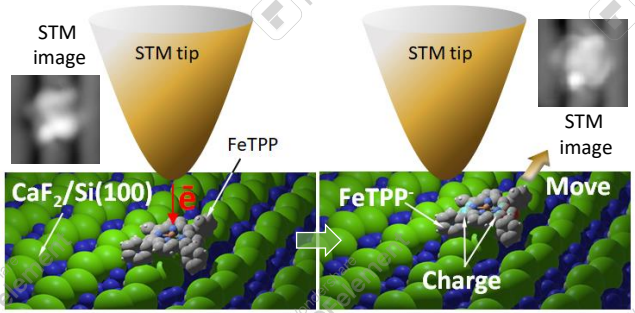

Duverger et. al

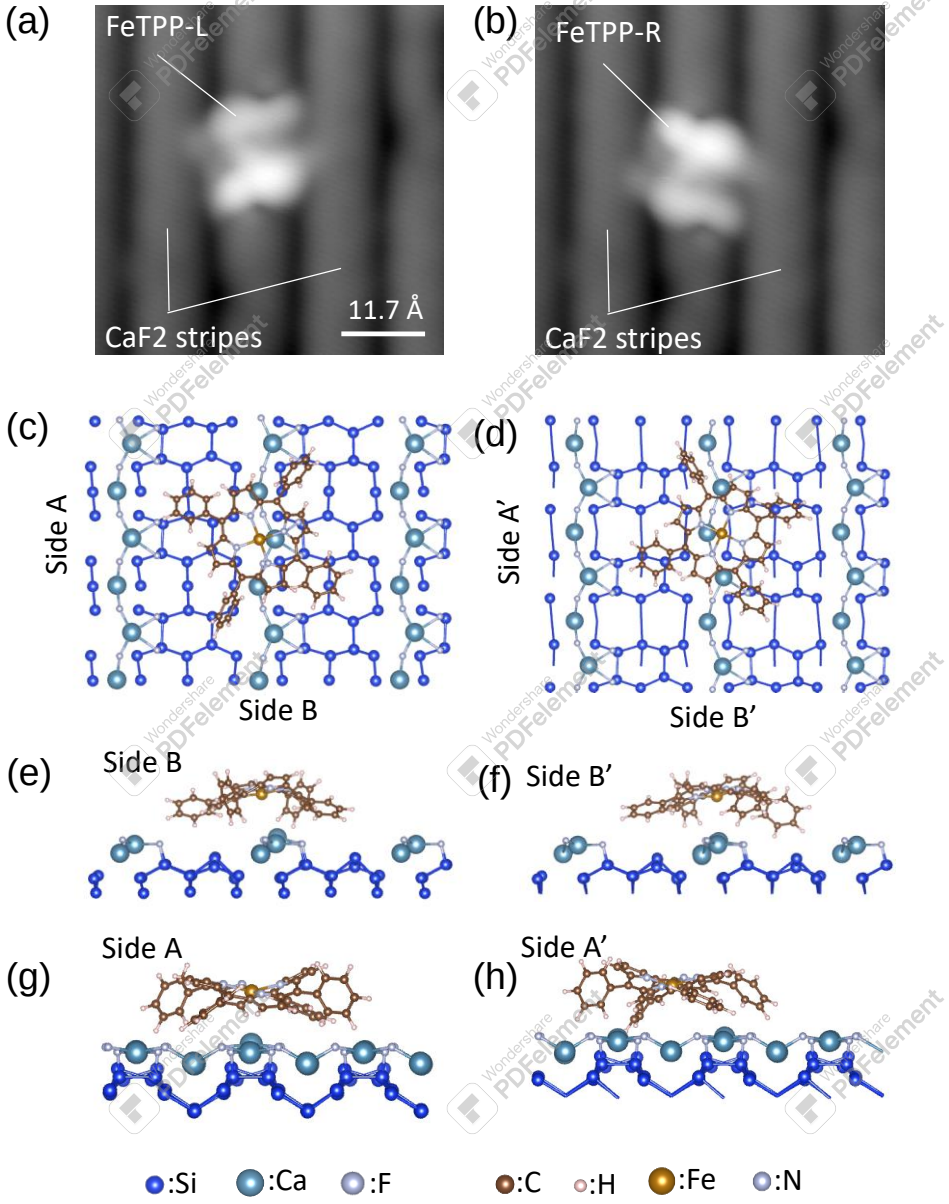

Duverger at al. Figure 1

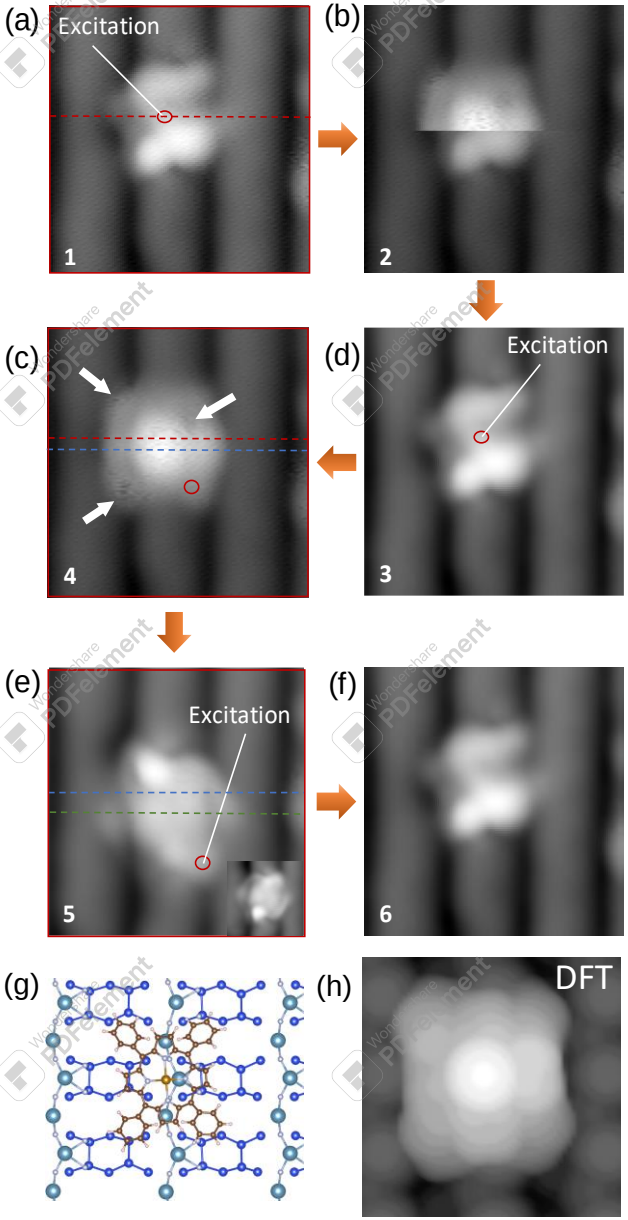

ACS Paragon Plus Environment

Duverger at al. Figure 2

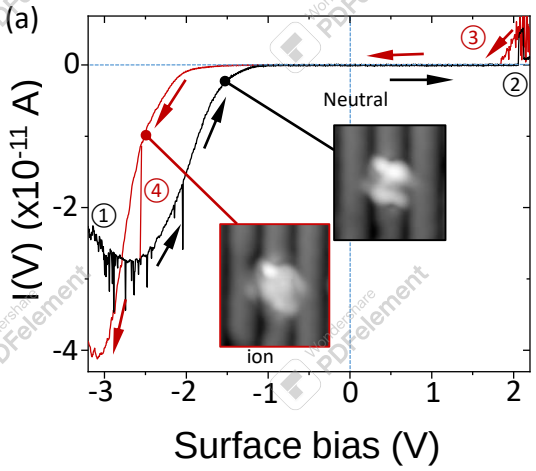

Duverger at al. Figure 3

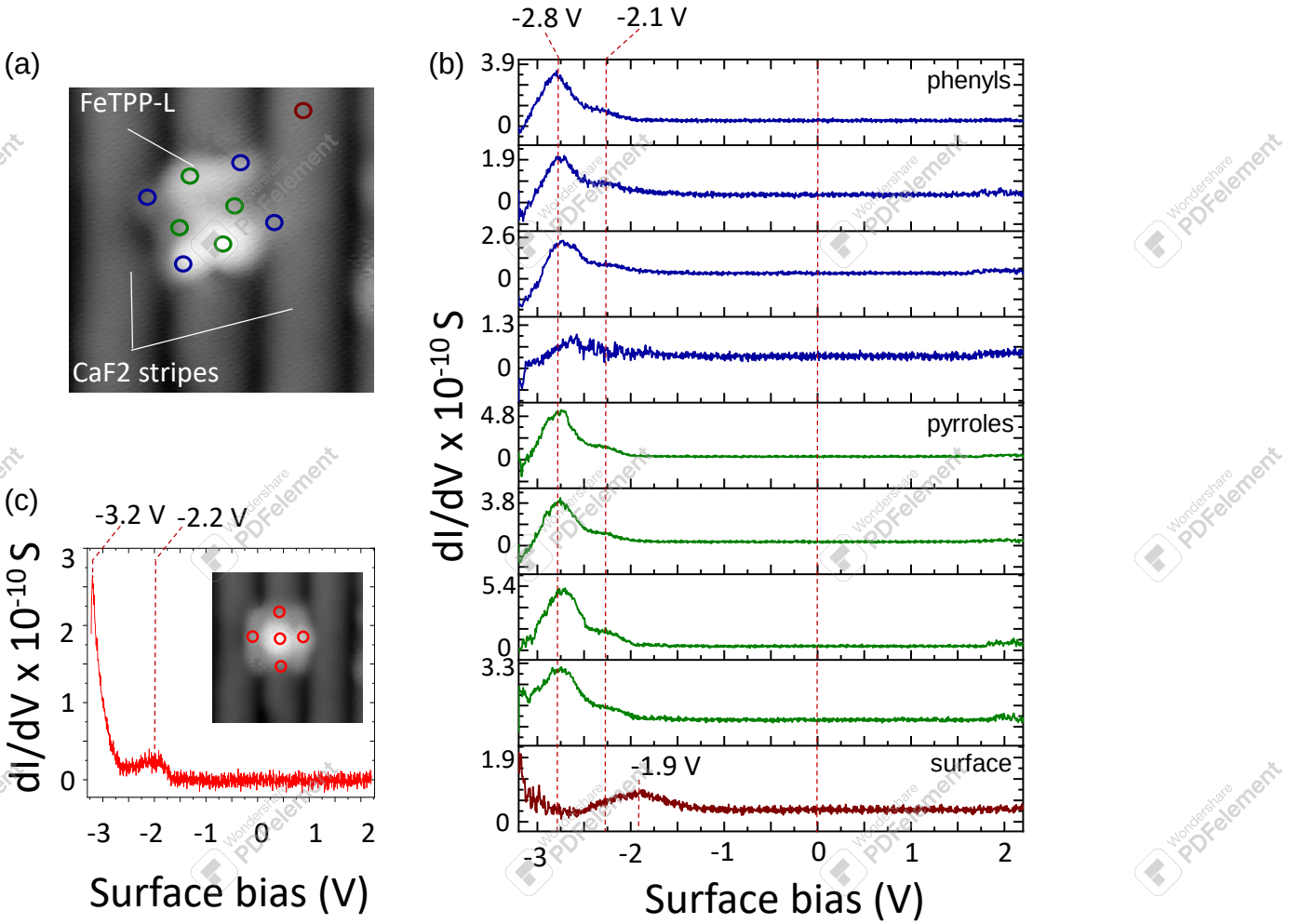

Duverger at al. Figure 4

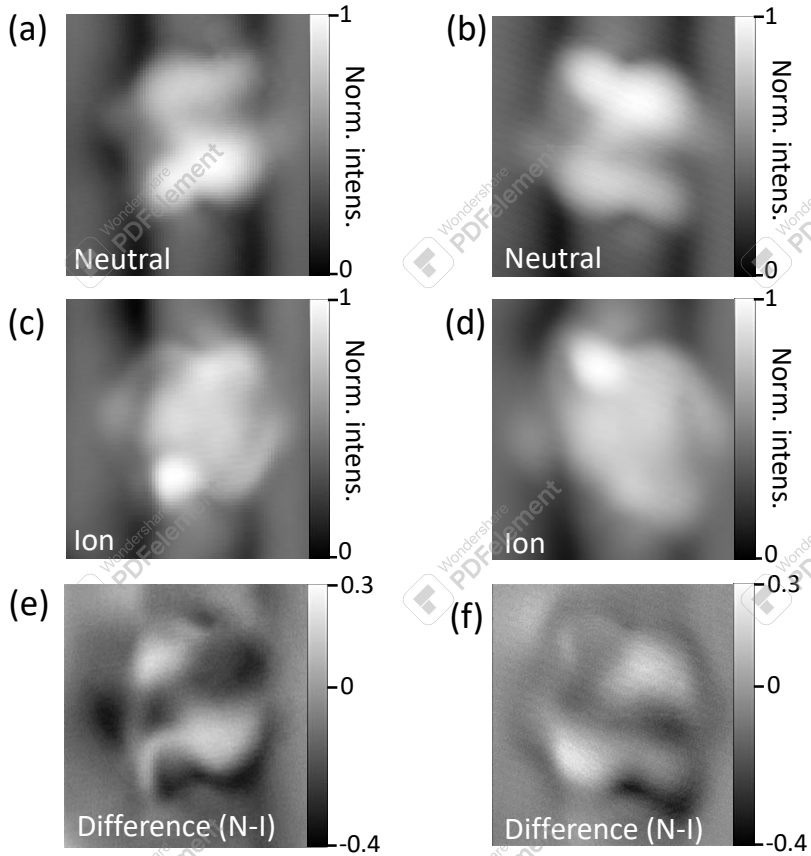

Duverger at al. Figure 5

(a)

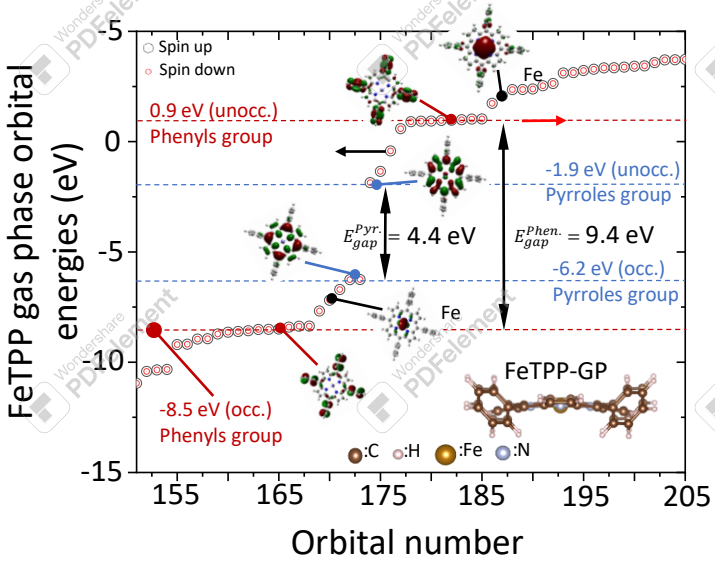

(b)

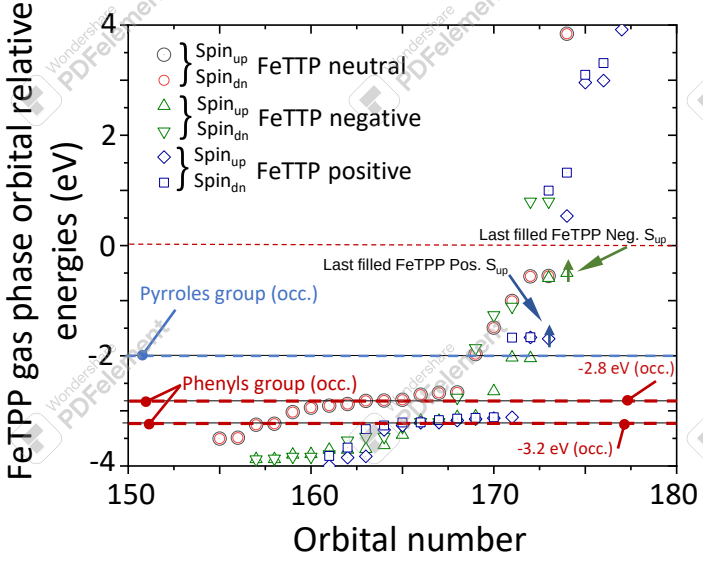

Duverger at al. Figure 6

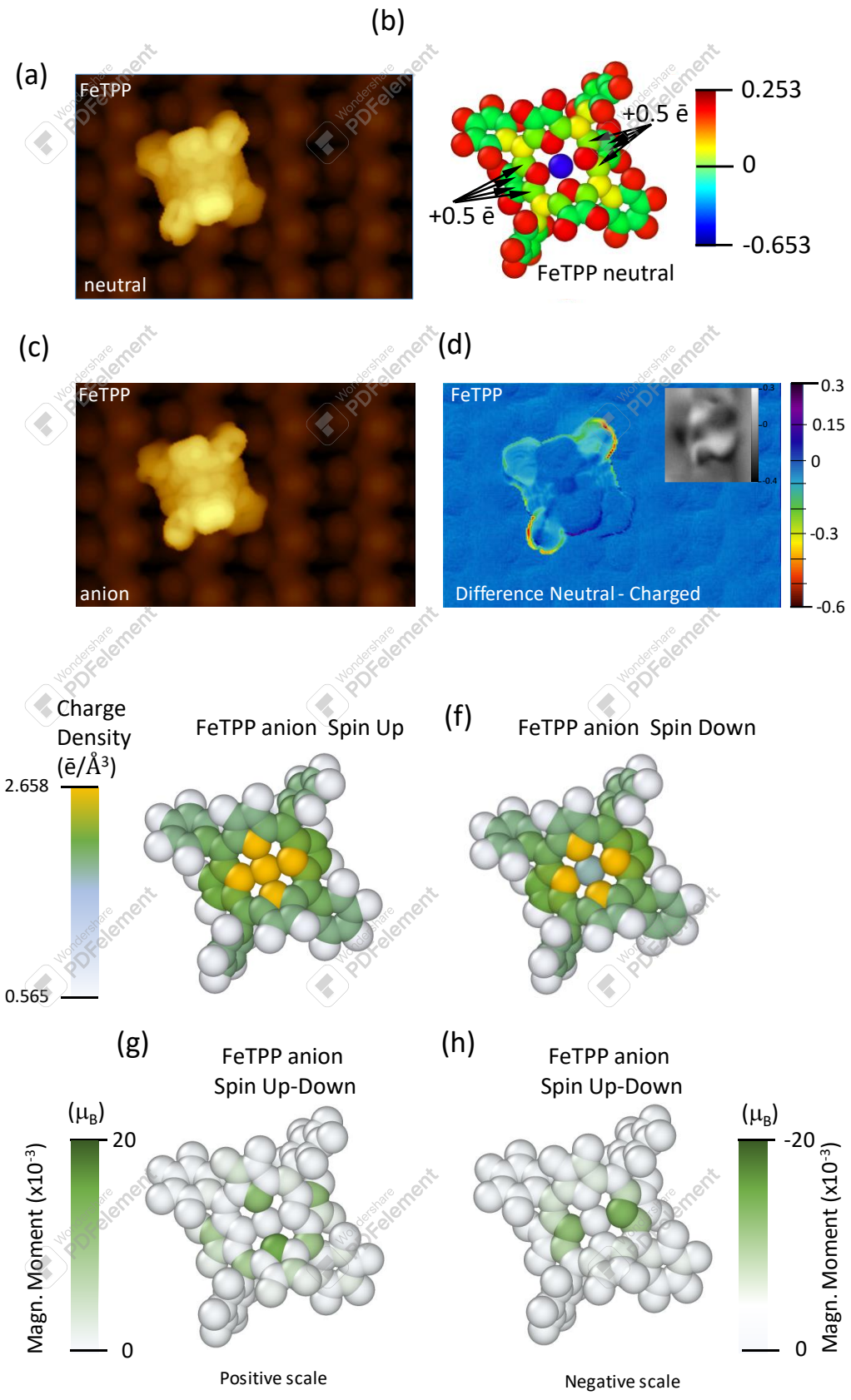

ACS Paragon Plus Environment

Duverger at al. Figure 7

Mapping the Reversible Charge State Control of an Iron Tetraphenyl Porphyrin Molecule Adsorbed on a CaF_2/Si(100) Semi-insulating Surface at Low Temperature (9 K)

Eric Duverger[1] and Damien Riedel[2*]

[1]*Institut FEMTO-ST, Univ. Bourgogne Franche-Comté, CNRS, 15B avenue des Montboucons, F-25030 Besançon, France*

[2]*Institut des Sciences Moléculaires d'Orsay (ISMO), CNRS, Univ. Paris Sud, Université Paris-Saclay, F-91405 Orsay, France. *:corresponding author*

Abstract :

This article presents a study concerning the charge state control of single iron-tetraphenyl porphyrins (FeTPP) molecules when adsorbed on a semi-insulating monolayer of CaF_2/Si(100) surface. The charge state of the FeTPP molecule is regulated by employing tunneling electrons from a low-temperature scanning tunneling microscope (STM) operating at 9 K. We show that once the charge is loaded into the FeTPP molecule, the molecule can be laterally manipulated across the surface without losing its charge state. The charge state change is reversible and the FeTPP molecule can be restored, at will, to its initial neutral state. A precise analysis of the STM topographies and dI/dV curves acquired on the FeTPP molecule before and after the electronic charge loading allows mapping the spatial charge state variations in the molecule as well as a conductance hysteresis effect, indicating the formation of an anion. Numerical simulation based on the density functional theory exploiting the virtual crystal approximation (VCA) method allows reproducing the trends of our experimental results and shows that the change in charge state affects specific areas of the molecule. Our theoretical investigations suggest that the molecular charge state variations can be monitored via STM topographies treatment and its local density of state distribution. This information can be related to the spatial distribution of the magnetic moment within the FeTPP molecule while the delocalization of the charge appears to depend on the total spin state of the central iron atom.

1. INTRODUCTION

Understanding and managing the charge state of individual atoms or molecules has been a longstanding challenge that has attracted considerable research attention for decades. This is because the charge state and its transfer at the nanoscale are known to govern numerous physical and chemical properties in nature[1]. When atoms or molecules are adsorbed on surfaces, the observation and control of charge state variations of adsorbates attract significant interest in both experimental and theoretical domains. Indeed, on surfaces, the charge state of adsorbates holds great significance in various contexts, including charge manipulation[2], molecular conformation[3,4,5], orbital entanglement[6], single-molecule Raman spectroscopy[7], solar cells[8], as well as molecular manipulation and energy transport[9,10]. These investigations typically require the use of local probe techniques such as scanning tunneling microscopy or atomic force microscopy, as they have proven to be highly efficient in controlling and measuring the charge state of adsorbates under various conditions[11]. In particular, local probe microscopy allows studying charge localization[12] as an important aspect to understand intermediate states[13] or charge memory effect in molecular assemblies[11,14]. In general, the analysis of an adsorbate's charge state can be determined by observing changes in conductance, as indicated by the characteristic shape of hysteresis[15]. In this context, the interactions between the surface states and the molecule are crucial for controlling the lifetime of the charge state[16]. Semi-insulating surfaces of various thicknesses, such as NaCl multilayers grown on Cu(111) and alumina (Al_2O_3) layers on NiAl surfaces, have been demonstrated to serve this purpose effectively. They have been utilized to control, map and investigate the evolution of the charge state of atoms or molecules in various ways[17,18]. Until now, the control and mapping of the charge state of molecules or atoms adsorbed on surfaces has not been observed on pristine semiconductor surfaces due to their very high chemical reactivity[19]. Yet, passivation of highly reactive silicon or germanium surfaces is known to hold the potential to provide such properties on a single atom, particularly when local dangling bond states can address various issues[20,21,11,22,23]. A particularly intriguing approach involves utilizing Si(100) epitaxy with a monolayer of CaF_2, as it facilitates an effective electronic decoupling between the surface and the adsorbate[24,25,26].

In this study, we illustrate the potential for inducing a reversible alteration in the charge state of a single iron-tetraphenyl porphyrin (FeTPP) molecule when it is adsorbed on a semi-insulating CaF_2/Si(100) monolayer surface at low temperature (9K). FeTPP molecule is a model molecule[27,28] often used to describe and study various physical and chemical processes in the gas phase or on surfaces such as charge transfer[29,30] spin transitions[31,32], catalysis[33,34], or photoactive devices[35,36].We employ a scanning tunneling microscope (STM) to inject electrons into the central part of the FeTPP molecule and subsequently image the different induced molecular charged states. The reversible nature of the charge states is elucidated through various effects, including the observation of hysteresis behavior in the time evolution of I(V) measurements, along with distinctive signatures observed in dI/dV spectroscopy. Furthermore, it is notable that the charge state of the FeTPP molecule remains steady when moved on the surface with the STM. By performing STM topographies difference between the neutral and charge states, we are able to map the stationary variations of the DOS migration related to the electronic charge loading. To deepen our comprehension of these discoveries, we employed density functional theory (DFT) calculations to elucidate the electronic structure alterations of FeTPP in its neutral, cationic, or anionic states. In this study, we employ DFT calculation methodology that exploits the virtual crystal approximation (VCA) based on a mixed atomic electronic structure to simulate the charge state of the FeTPP molecule on a surface. This approach enables us to replicate the trends observed in our experimental results, including differences in STM images, and provides insights into the influence of the initial FeTPP electronic structure and spin state. Our findings demonstrate the ability to effectively generate a FeTPP anion by introducing negative charges, facilitating its transport across the surface through ad-hoc excitation, and subsequently restoring the FeTPP molecule to its neutral state. This paves the way for the exploitation of such adsorbates as a nanoscale electron reservoir.

2. METHODS

2.1 Sample and tip preparation

The fabrication of the ultrathin semi-insulating layer is performed in two steps. The first step consists of preparing the reconstruction of the Si(100) surface (n-doped (As), ρ = 5 Ω·cm) through

several cleaning cycles in ultrahigh vacuum using repetitive annealing series. This entails a swift temperature rise up to 1100 °C, succeeded by a gradual temperature decrease to 600 °C. The subsequent step encompasses the epitaxial growth of the reconstructed Si(100) surface: Si(100)-2x1 is exposed to a flux of CaF_2 molecules evaporated from an effusion cell heated to 1065 °C, while maintaining the Si sample at a temperature of 720 °C[37]. The CaF_2 exposure lasts for 120 s, providing a total coverage of approximately 1.3 monolayers. During the CaF_2 exposure, the pressure in the preparation chamber is maintained below 2×10^{-10} torr. Following this procedure, the sample is cooled down to 12 K and then withdrawn from facing the CaF_2 oven. The CaF_2 oven made of pyrolytic boron nitride (PBN) is subsequently cooled down to approximately 500 °C to prevent spurious evaporation. Then, the FeTPP molecules powder is heated in the oven (PBN) until it reaches its sublimation temperature, at approximately 250 °C. Once the FeTPP molecules are sublimated, the CaF_2/Si(100) sample is positioned in front of the oven for approximately 2 seconds. At the end of this procedure, the sample is gradually cooled down to 12 K and then introduced into the STM chamber for analysis. The characteristics of the obtained semi-insulating layer structure and properties have been detailed in previous research[24,37].

The STM tips are crafted using a tungsten wire that undergoes electrochemical etching in a sodium hydroxide (NaOH) solution and then cleaned by exposure to electrons within the ultra-high vacuum (UHV) preparation chamber. The scanning tunneling spectroscopy (STS) curves obtained in our experiments arise from two lock-in amplifiers. The results are compared to avoid spurious dI/dV peaks and to reduce background noise. During the STS measurements, an amplitude modulation of 5−10 mV at a frequency of 847 Hz is applied to the sample in addition to the constant bias voltage. The tunnel current is converted to a voltage signal outside the STM chamber, with a noise level below 7 mV, ensuring a robust average signal-to-noise ratio on the measured (dI/dV) signals. Throughout the measurement process, we collect (dI/dV) curves at different STM tip height positions to assess potential energy shifts in the density of state (DOS) peaks. These shifts can be due to band-bending effects caused by the STM tips or voltage drop occurring at the double barrier junction. All measurements are performed with a low-temperature (9 K) PanScan STM head from CREATEC at a base pressure below 10^{-12} torr. The bias voltage is applied to the silicon sample, and the excitation pulses applied to the molecule are statistically analyzed (see Fig. S1), confirming the electronic nature of the charge state

change. The average time required to induce the charge state modification of a FeTPP molecule is estimated ~ 0.46 ± 0.05 s, resulting in an electronic yield $Y_{ion} = 1.16 \times 10^{-8} \pm 0.1\ \bar{e}^{-1}$.

2.2 Theoretical methods

Calculations of the FeTPP's electronic structure in the neutral and charged states are carried out in several steps. The initial step involves employing the Gaussian 09 software package[38] to simulate the relaxation of the FeTPP molecule in its different neutral and charged states in the gas phase. The considered spatial structure of the FeTPP molecule is either the one that has been relaxed on the surface or a fully relaxed structure using the self-consistent field SCF optimization method. As a second step, we have also performed numerical simulations of the FeTPP molecule when adsorbed on the epitaxial CaF_2/Si(100) surface by using the Spanish Initiative for Electronic Simulations with Thousands of Atoms (SIESTA) package[39,40,41,42]. The various FeTPP molecular electronic structures are thus investigated through numerical simulations using the density functional theory (DFT) method. In these simulations, we employed a polarized double-ζ basis set (DZP) and nonlocal norm-conserving pseudopotentials. For the exchange-correlation functional, we adopted the generalized gradient approximation (GGA) that includes van der Waals interactions[43,44,45].

To achieve high precision in calculating the total energies of the studied systems (1 meV), we utilized a mesh cutoff of 150 Ry and a single k-point at the center Γ for Brillouin zone integration. Geometry relaxation was accomplished using the conjugate-gradient method with a force convergence criterion of 0.02 eV/Å. This process was conducted while maintaining the volume of the identical slab, characterized by dimensions of 4.64 × 3.10 × 4.44 nm³. The volume corresponds to the CaF_2/Si(100) slab and includes a total of 1293 atoms, counting those of the FeTPP molecule. Precise localization of the FeTPP molecule on the CaF_2/Si(100) surface was achieved with reference to previous work[24]. The final molecular conformation is optimized based on criteria related to minimizing the conformational adsorption energy and our ability to reproduce experimental STM images. To achieve this, we applied the Tersoff-Hamann approximation method to generate a map of the isodensity of surface states by calculating the local density of state (LDOS) within the calculated energy window. In order to describe the anionic electronic state of the FeTPP molecules adsorbed on the CaF_2/Si(100) surface, with the

charge added either to the Fe atom or at other locations in the molecule, we exploit the virtual crystal approximation (VCA) as implemented in SIESTA[46]. This method relies on creating one or more virtual atoms by combining known reference atomic pseudopotentials, originally provided by SIESTA, and averaging matrix elements in Fourier momentum space. The nuclear charge of the pseudo-atom is adjusted to maintain the atomic charge neutrality. Through this approach, the Mixps code integrated into SIESTA allows for the adjustment of the nuclear charge of the pseudo-atom. This procedure includes a description of the initial neutral Fe (or C) valence electrons as $4s^2\ 3d^6$ ($2s^2\ 2p^2$). With an additional electronic charge value 'x', the electronic structure is represented as Fe (C): $4s^2\ 3d^{6+x}$ ($2s^2\ 2p^{2+x}$), where x can range from -0.9 ē to 0.9 ē. *The resulting stationary charge state distribution is analyzed throughout the entire slab using the Bader approach [47]. With a highly precise grid sampling coupled with an ad hoc Voronoi volume definition, our calculation can achieve precision as fine as 2 x10^{-3} ē [48,49,50].*

It's important to emphasize that substituting an iron atom, initially carrying a nuclear charge of 26 protons, with a virtual species created as a mix of two different atoms' pseudopotentials, results in a modification of the total number of protons to 26 + x. This implies that the VCA method does not merely result in a variation of the additional charge by x valence electrons, as the Coulomb attraction between the additional charge and its nucleus might retain some of the added charge in close proximity to the mixed atom's position during electronic optimization. Therefore, we have observed that a significant fraction of the partial negative charge behaves in a quasi-free manner, becoming delocalized through local fluctuations in the electrostatic potential. This leads to a satisfactory reproduction of the stationary charge state variation trends of the considered molecule.

3. EXPERIMENTAL RESULTS

The FeTPP molecules adsorb on the CaF_2/Si(100) surface in two main configurations that have already been studied in previous work[51,24]. Their STM images are depicted in Figs. 1a and 1b, illustrating two different orientations referred to as FeTPP-L and FeTPP-R. These orientations occur when the molecule is angled approximately ± 23° to the left or right, respectively, compared to the direction of the CaF_2 stripes[51]. *Figs 1c to 1h illustrate the relative physisorbed conformational positions of each*

adsorption site on top of the CaF_2/Si(100) surface. The FeTPP molecules are known to be physisorbed on the CaF_2/Si(100) semi-insulating surface, demonstrating minimal interaction with the substrate[24]. *Our former work details the description of the FeTPP interactions with the CaF_2/Si(100) surface leading to a molecule-surface distance at the central Fe atom of ~ 5.4 Å.* In this context, the formation and lifetime of adsorbates excited states, including ionic states are favored[16]. Our study uses the principle of electronic excitation to induce charge state modification in the adsorbate with a minimum of conformational change[52,53,54,55]. This procedure is elaborated in detail in the method section, building upon prior research[23]. Here we set specific parameters for this process in order to test our ability to create a stable ionic state in the molecule. In particular, we aim to fabricate stationary FeTPP ion and see if this electronic state can be observed on the surface with the STM and for how long. Our tests start on a FeTPP-L molecule on which is applied a voltage pulse ($V_{exc.}$ = + 2.5V, 6 - 10 s) at the center of the molecule (red circle in Fig. 2a, #1). We observe the result of this excitation by scanning the exact same surface area (Fig. 2b, # 2). The ensuing STM topography, as the scan occurs from the upper part to the lower part of the image, exhibits a conformational change from the previous image that suddenly changes in the second half of the picture. A careful look at Fig. 2b shows that the second part of the STM topography resembles the initial FeTPP molecule in its FeTPP-L conformation, indicating that the molecular conformational change in Fig. 2b is reversible and somewhat slightly unstable under our scanning conditions (-2.3 V, 7 pA). It is important to notice that during the electronic excitation pulse applied on the molecule in Fig. 2a, the bias voltage is positive, implying that the tunnel electron flux migrates from the STM tip, through the molecule, and then to the surface. Under these conditions, the tunneling electrons primarily explore the empty states of the molecule, thereby enhancing the likelihood of forming an anion. Hence, when the bias voltage is negative during the scan in Fig. 2b, the tunnel electron flux is reversed (i.e. from the surface to the STM tip) increasing the probability to neutralize the FeTPP molecule. After a third scan of the identical region (Fig. 2d, #3) that distinctly demonstrates the recovery of the FeTPP molecule to its initial conformation, as depicted in 2a, we apply the same excitation pulse on the central part of the FeTPP molecule. The subsequent topography (Fig. 2c, # 4) shows the entire configuration of the FeTPP molecule after the excitation. One can recognize that the first upper half part of the image in panel 2b resembles the spatial repartition of DOS observed in panel

2c. It is also possible to detect strong differences, apart from a possible molecular conformational change, between the STM topography of the neutral FeTPP molecule (Fig. 2a) and the one imaged in the panel 2c. Indeed, the texture and corrugation of the spatial distribution of the excited molecule, as observed in Fig. 2c, appear noisier. This suggests that the conductivity through the DOS of the molecule is somewhat reduced at multiple locations (see white arrows in Fig. 2c). Earlier studies on FeTPP molecules on the CaF_2/Si surface have revealed that applying excitation with a negative bias voltage to the phenyl groups of the molecule effectively triggers its movement from the FeTPP-L to the FeTPP-R conformation[29]. This transition is commonly accompanied by a displacement of the molecule along the stripe. This shift is evident when we overlay the red dotted line passing through the central region of the neutral FeTPP-L molecule from Fig. 2a onto Fig. 2c. In contrast, the blue dotted line in Fig. 2c intersects the midpoint of the newly adopted FeTPP conformation. Note that low-temperature scanning tunneling microscopy (STM) allows for the recording of STM topography of the same surface area with negligible lateral drift. An excitation pulse at negative bias voltage ($V_{exc.}$ = - 2.5 V, 6-10 s) is then applied at the position of the lower right phenyl group on the FeTPP molecule (see red circle in panel 2c). One can report to previous work to further understand the mechanism induced when an excitation pulse is applied at negative bias voltage to control the FeTPP movement over the CaF_2 stripes[51]. The subsequent STM topographic image of the identical region (Fig. 2e, # 5) is striking, revealing the FeTPP molecule in what appears to be a slightly different conformation. This molecular configuration bears strong resemblances to the FeTPP-R depicted in Fig. 1b, featuring a similar rightward rotation at the same angle relative to the axis of the CaF_2/Si(100) stripe. However, the spatial distribution of the FeTPP DOS shown in Fig. 2e is significantly different from the one in Fig. 2a, while the general contour is kept. We also note that the molecule in this conformation has been slightly shifted downward along the CaF_2 stripe, in coherence with the known effect of excitation at negative bias voltage. The blue dashed line, which crosses the center of the molecule in Fig. 2c, is indicated in Fig. 2e for comparison with the position of the center of the FeTPP molecule conformation, denoted by the green dashed line. This result indicates that the FeTPP molecule, likely existing in a specific ionic state in Fig. 2c, can move on the surface while maintaining its specific electronic charge state. An additional excitation pulse at negative voltage ($V_{exc.}$ = - 2.5V, $T_{exc.}$ = 10 s) is then applied on the lower right phenyl group of the ionic FeTPP molecule (red

circle in Fig. 2e). This final excitation can either provoke the movement of the FeTPP molecule along the CaF_2/Si(100) stripe (inset in Fig. 2e) or to return to its initial state (Fig. 2f) like the one seen in Fig 2a, indicating that the neutralization of the ionic FeTPP molecule can also be achieved via an electronic excitation at negative bias. Note that the ionic state of the FeTPP molecule as observed in Fig. 2e (and inset) is stable for several hours. Calculation of the relaxed structure of the FeTPP as observed in Fig. 2c is performed and shown in Fig. 2g. The ensuing calculated local DOS is provided in Fig. 2h with good reproducibility.

To further study the charge state of the ionic FeTPP molecular conformations observed in Figs. 2e, we have performed I(V) measurements on a neutral FeTPP molecule with a bias voltage varying from -3.1 V to 2.2 V and vice versa (Fig. 3) to observe a possible hysteresis behavior. For this measurement, the STM tip is located on top of the Fe atom of the neutral molecule and the applied bias is tuned, starting at a bias voltage of -3.2 V (point ① in Fig. 3). The evolution of the I(V) (black curve) reaches a maximum at -2.6 V to decrease down to 0 A at Vs ~ -1.2 V. The tunnel current remains null up to a bias voltage value of 2 V due to the large surface gap energy of the CaF_2/Si(100) surface of ~ 3.2 eV[24,26,37]. The I(V) curve switches suddenly to a higher value and becomes very noisy when the current establishes at positive voltage (point ② in Fig. 3), sign of a strong molecular transient change. When the bias voltage is swept back to -3.2 V (red curve in Fig. 3) the tunnel current value decreases rapidly to 0 A until the bias reaches -1.5 V. Hence, the ensuing I(V) curve does not follow the previous black curve, shifting the I(V) maximum to a lower value at ~ -3.1 V. In some cases, the I(V) red curve switches back to the black curve within a range of voltage ~ 2.5 V (point ④ in Fig. 3). In the presented case, scanning the same area of the FeTPP molecule after an I(V) measurement sequence indicates that the molecule resembles the conformation observed in Fig. 2e. This result reveals that the charge state of the FeTPP molecule has changed when the bias voltage applied is positive while the general conformation of the FeTPP and its position on the surface remain nearly the same. Consistently, given the chosen experimental parameters for the investigations presented in Fig. 2 and Fig. 3, it can be anticipated that the change in charge state would result in the formation of a specific anion.

For a better comprehension of the electronic structure changes induced by the formation of an ionized FeTPP molecule, it is necessary to compare the variations of DOS between a neutral and ionized molecule. This can be performed by analyzing the dI/dV curves acquired at several selected positions in the FeTPP molecule as presented in Figs. 4a and 4b. The dI/dV curves in Fig. 4b exhibit very similar variations of DOS peaks whether they are acquired on top of a pyrrole group or on top of a phenyl group (see the green and blue circles and ensuing curves in Figs 4a, 4b, respectively). The main DOS peaks are observed at -2.8 V with a shoulder at ~ -2.1 V. These two DOS peaks can be attributed to the phenyl groups (-2.8 V) and the pyrrole groups of the FeTPP molecule. In its neutral configuration, FeTPP-L (or FeTPP-R) features a relative orientation of the aromatic phenyl groups surrounding the porphyrin macrocycle, enabling the adjustment of electronic coupling with the pyrrole groups through their dihedral angle. This can be expressed by a more or less intense delocalization of the DOS peaks associated with each chemical group throughout the molecule. Consequently, this effect leads to similar spectroscopic curves across the neutral FeTPP-L and FeTPP-R molecules, as demonstrated by the dI/dV data in Fig. 4b. A further important signature indicating that the FeTPP molecular occupied states can be considered as decoupled electronically from the surface is evidenced by the CaF_2/Si(100) surface DOS peak at lower energy (-1.9 eV).

Interestingly, the dI/dV spectroscopy acquired on the ionized FeTPP molecule (Fig. 4c), shows key differences compared to the one acquired from the neutral molecule. The first difference arises from a general shift of the occupied DOS to lower bias values. One can notice that the DOS peak ascribed to the pyrrole groups, initially located at -2.1 V for the neutral FeTPP molecule, is observed at a very similar voltage for the FeTPP ion (-2.2 V). However, the DOS peak associated to the FeTPP phenyl groups is significantly shifted to a lower bias (-3.2 V), in line with the observation in the I(V) curve where a peak of current at similar bias is observed (Fig. 3). This effect is consistent with a decrease in the total energy of the FeTPP molecule due to the additional electronic charge, which may further stabilize its electronic structure. This result confirms our first hypothesis suggesting that both FeTPP configurations observed in Figs. 2c and 2e are stationary STM images of the FeTPP anion. Furthermore, the relatively large voltage shift of the DOS peak at -3.2 V suggests that the charge variation of the FeTPP molecule may strongly affect the phenyl groups of the molecule. This assumption is surprising

because the electronic excitation is initially applied locally to the central part of the molecule, i.e., to the Fe atom whereas it appears to influence the whole electronic structure of the molecule. Here, it is important to emphasize that the DOS tail observed in the dI/dV curve acquired on the CaF_2/Si(100) surface (red curve in Fig. 4b) does not show the same maximum as the one observed on the ionized FeTPP molecule (Fig. 4c). A clear comparison of the two measurements is provided in Fig. S6.

To delve deeper into the alteration in charge state and its impact on the spatial distribution of DOS, we conducted experimental comparisons of the constant current image isodensity between the FeTPP-L and FeTPP-R conformations, alongside STM images in their corresponding conformations while in the anion state (Figs. 5a to 5d). To compute this intensity difference, we chose STM images of identical dimensions (256 x 256 pixels) where both FeTPP molecular states are positioned precisely the same and exhibit identical intensities. To avoid spurious analysis, while each STM topographies are performed with the same STM parameters (V_s = -2.8 V, I = 7 pA), and to warrant the same STM tip height, the image profile grayscale is normalized so that the resulting contrast will arise from a pure variation of DOS. We are also assuming that the transition between two different charge states, from the neutral FeTPP (depicted in Figs. 5a, 5b) to the anionic FeTPP (shown in Figs. 5c, 5d) does not cause significant conformational changes that could involve large atomic displacements. In this context, we consider that when the FeTPP molecule is ionized, the STM picture of each molecular state, i.e. neutral or negatively charged, is the stationary result of a redistribution of the charge density change, all over the molecule. This redistribution arises from an electronic structural reorganization due to the addition or removal of partial electronic charge. With these assumptions, we based our approach of the STM image difference as a method to describe the spatial redistribution of DOS between a neutral and an ionized molecule.

The STM topographies differences (i.e. FeTPP neutral image minus FeTPP anion image) are shown in Figs. 5e and 5f for the FeTPP-L and FeTPP-R, respectively. In these figures, the dark gray areas indicate where the DOS difference is negative, i.e. where the DOS intensity of the neutral FeTPP is lower than the anion FeTPP DOS. In both images (Figs. 5e, 5f) the dark areas are rather located in the middle part of the molecule, spreading aside each lateral pyrroles group of the macrocycle. In addition, the upper right and lower left phenyl rings of the molecule seem to be also affected as well by the DOS

redistribution as they show a negative difference. Inversely, the bright areas illustrate where the neutral FeTPP DOS intensity is higher than the anion FeTPP DOS. These zones are rather located at the upper and lower pyrroles group.

Each pixel in the STM topography is proportional to the integration value of all the DOS, covering the energy range from the Fermi level energy of the STM tip to the Fermi level energy of the CaF_2/Si(100) surface. As a result, a negative change in DOS indicates the migration of the averaged DOS from the neutral molecule configuration to the anion molecule configuration. We can infer that the additional electronic charge in the FeTPP molecule becomes redistributed across specific parts of the molecule, despite being initially concentrated at the Fe atom upon injection by the STM tip. At this point, it cannot be discounted that there may be some minor atomic position variations to accommodate the molecular structure in this new charge state[56,57].

4. DISCUSSION

To understand our experimental results, we conduct numerical simulations of the electronic structure of a neutral FeTPP molecule in the gas phase and for various charge states (Fig. 6). In Fig. 6a, we depict the Kohn Sham (KS) orbitals energies of the neutral FeTPP molecule in the gas phase. Upon calculating the electronic structure of the FeTPP molecule in the gas phase, it becomes clear that the few frontier orbitals are primarily composed of DOS localized mainly at the macrocycle porphyrin, resulting in a molecular HOMO-LUMO gap energy of ~ 4.4 eV (see blue lines at -6.2 eV and -1.9 eV). The FeTPP molecule's electronic structure is also composed of two groups of a tenth of KS orbitals having very similar energies at the occupied and unoccupied states for which the DOS is mainly localized at the phenyls groups (i.e. red lines at -8.5 eV and 0.9 eV, respectively). The energy difference between these two DOS peaks is 9.4 eV for the molecule in the gas phase. It is important to note that, for the metallated molecular porphyrin family, the energy difference between the occupied and unoccupied phenyl groups is often mistaken for the HOMO-LUMO energy gap of the molecule, whereas the actual frontier orbitals are shown to exist at lower energies. *A detailed comparison of the Kohn Sham (KS) orbitals energies of*

the neutral FeTPP molecule in the gas phase with the projected DOS calculated with the FeTPP molecule adsorbed on the CaF_2/Si(100) surface is provided in Fig. S7.

To illustrate the impact of the charge state alteration subsequent to FeTPP excitation and to confirm whether the FeTPP molecule indeed behaves as an anion rather than a cation, we conducted spin-polarized calculations of the electronic structure of the FeTPP molecule in the gas phase, under neutral, negative, or positive charge conditions, and compared the results with the experimental dI/dV curves depicted in Figure 4. This finding is illustrated in Fig. 6b, where the energy of the occupied state of the phenyl groups serves as reference energy, thereby adjusted to align with the energy of the dI/dV curves measured in Fig. 4. Therefore, the occupied state energy of the phenyls group orbitals (red and black circles in Fig. 6b), initially lying at -8.5 eV (Fig. 6a), is adjusted to match the energy value of the phenyls dI/dV peak acquired on the neutral FeTPP molecule (Fig. 4b). Next, a similar energy adjustment is applied to the calculated orbital energies of the negatively or positively charged FeTPP molecule, depicted by the green and blue symbols in Fig. 6b, effectively setting the occupied orbitals of the phenyl group at -3.2 eV as a reference energy of the ensuing dI/dV curve. This method allows for comparing the calculated orbitals situated at higher energies to determine if they correspond to the dI/dV curves of the resulting pyrroles DOS peaks measured experimentally. A thorough comparison can be found in Fig. S8.

Fig. 6b reveals, firstly, that the variation in charge state of the FeTPP molecule primarily affects the electronic structure of the frontier orbitals associated with the pyrrole groups in the range spanning from 0 to -2 eV as well as the tail of the phenyls KS orbitals ranging from -2 to 3 eV. The trend revealed by these calculations also indicates that the dI/dV peak tail attributed to the pyrrole group represents only a portion of the frontier orbitals. This is evident as the energy of the calculated HOMO orbital of the neutral FeTPP molecule is approximately - 0.5 eV. This effect is primarily attributed to the insulating properties of the CaF_2/Si(100) layer, which significantly reduces surface conductivity for surface biases greater than -1.5 V and below the surface Fermi level energy. It is therefore relevant to compare the ensuing energy of the HOMO orbital with the voltage drop ∘ V that generally occurs in double junction barriers where $\gamma = d/(\varepsilon z + d)$[58]. Under our experimental conditions, we can roughly estimate that the voltage drop is lower than 0.1 V at -2.5 V when the tip-to-molecule distance z = 10 Å, the CaF_2 insulating

thickness d is ~ 1 Å[24] *, and the dielectric constant ε of the insulating layer is about 8. This estimation* supports our earlier observations.

Since the cluster of orbitals associated with the occupied phenyl groups are deliberately set to have similar energy levels for both negatively and positively charged FeTPP molecules in order to compare them, one can then examine the corresponding energies of the orbitals in the ensuing pyrrole groups. For the positively charged FeTPP molecule, the calculated last filled occupied orbitals of the pyrrole groups have energies located at approximately -1.7 eV. In contrast, two spin-up states with filled orbitals from the pyrrole groups of the negatively charged FeTPP molecule are observed at -2.0 eV, along with two other orbitals at around -0.5 eV. By comparing the dI/dV curves obtained for both the neutral FeTPP and the ionized FeTPP molecule (Figs. 4b, 4c) with the calculated orbital energy lines for both the neutral and ionized forms of the molecule, a discernible pattern emerges. It becomes clear that the electronic structure most closely mirroring the acquired spectroscopic curve corresponds to the FeTPP anion. Indeed, the first set of orbitals of the negatively charged FeTPP molecule lying at -2.0 eV can be clearly observed in the dI/dV measurements. However, the last filled orbitals at -0.5 eV cannot be measured due to the surface gap of the CaF_2/Si(100) surface.

These results further indicate that the electronic excitation of the FeTPP molecule results in a negatively charged state and that its electronic structure is very similar to the FeTPP anion. It is important to emphasize here that only the energies of the occupied orbitals are compared since the HOMO-LUMO gap energy may change once the molecule is adsorbed on the surface. Our calculations also enable the estimation of the ionization potential energy (IP) of the gas-phase conformation of the FeTPP molecule by applying the Koopman theorem. Thus, the ionization potential $IP = E_{cation} - E_{neutral} = 6.5$ eV, as well as the electronic affinity $Ea = E_{neutral} - E_{anion} = 2.8$ eV. Although these values of IP and E_a energies may decrease for the physisorbed FeTPP molecule on the CaF_2/Si(100) surface, this strongly suggests that the formation of a long-term stable electronic state for the FeTPP anion is more easily achieved compared to the cationic form.

When acquiring one (or more) additional electron in the neutral FeTPP molecule to form an FeTPP anion, several transient electronic changes may occur. Specifically, in our experimental excitation methods, the STM tip is positioned above the Fe atom, suggesting a higher probability of

localizing the additional electronic charge on this atom initially. However, as depicted in Figs. 5, the static variation of charge density in the FeTPP molecule before and after the formation of the anion primarily affects not only the central part of the molecule but also the surroundings of the porphyrin macrocycle. Therefore, it is crucial to describe how the additional electronic charge is distributed in the FeTPP molecule before and after the electronic excitation.

To further describe this effect, we have calculated the LDOS of a neutral FeTPP molecule adsorbed on the CaF_2/Si(100) surface (Fig. 7a). As depicted in Fig. 7b, the ensuing Bader charge variation analysis of a neutral FeTPP molecule indicates that the iron atom in the neutral FeTPP has lost 0.653 ē (blue sphere) compared to its initial valence charge state (Fe:$4s^2$ $3d^6$), while the surrounding nitrogen atoms gain additional charges of ~ 0.243 ē compared to its initial valence charge state (N: $2s^2$ $2p^3$, red spheres). We then proceed to modify the initial electronic structure of the neutral FeTPP by adding 0.5 electronic charges to the four carbon atoms of the two lateral pyrrole groups (Fig. 7b) to mimic what is observed in Fig. 5e. The visual impact of the additional charges on the LDOS of the FeTPP molecule is relatively subtle, as observed in Fig. 7c, although some minor differences are already noticeable at the lower left and upper right phenyl rings of the molecule. To emphasize the LDOS variations between Fig. 7a and 7c, we compute the difference between the two LDOS distribution images and present the results in Fig. 7d. This reveals clear LDOS variations in relation to the additional charge initially located at the lateral pyrrole groups. Indeed, upon comparison with the subsequent experimental STM image difference presented in the upper corner of Fig. 7d, one can readily observe that the two lateral pyrrole groups, along with three surrounding phenyl groups, display negative variations in LDOS (Fig.7d), aligning with experimental observations. Similarly, the LDOS difference at the upper and lower pyrroles groups stays positive or near zero. This implies further similarities with our experimental STM image processing technique, suggesting that the additional charge is delocalized in the regions where the LDOS difference is negative.

Given that the FeTPP molecule can initially undergo spin polarization via a magnetic moment primarily localized at the iron atom, it is relevant to investigate how the delocalization of the additional added charge in the FeTPP molecule anion may correlate with a variation in the magnetic moment of the entire molecule. As depicted in Figures 7e and 7f, at first glance, the discrepancy in the spin-up and

spin-down FeTPP anion Bader charge distribution may not be immediately evident and seems uniform across all atoms of the molecule, except for the central Fe atom. In particular, there appears to be a more pronounced variation of spin-up charge at the Fe atom (i.e. 2.6 $\bar{e}$ ↑) compared to the spin-down (i.e. 1.6 $\bar{e}$ ↓) while the additional charge is initially introduced into the carbon atoms of the two lateral pyrrole groups. Therefore, the local spin magnetic moment of the FeTPP anion worth 0.82 μ_B (μ_B being the Bohr magneton).

Calculating the differences of the spin polarized charge variation per atom enables mapping the local magnetic moment of the molecule on each atom of the FeTPP molecule, as depicted in Figs. 7g and 7h. To optimize the color scale, the charge difference values at the Fe atom is set to zero. One can observe that the most significant values of positive magnetic moment (i.e., 18 mμ_B) are located on the two nitrogen atoms forming the upper and lower pyrrole, with only minor effects on the other atoms of the molecule. However, the negative magnetic moment values (i.e., -13 mμ_B) are primarily distributed among the nitrogen and carbon atoms in the lateral pyrrole groups located on the left and right sides of the molecule. This reveals a specific reorganization of the electronic spin state over the entire FeTPP molecule to stabilize the extra charge and the ensuing variation of the local magnetic moment of the Fe atom.

Given that the process for loading the molecule with additional electrons occurs at the central part of the molecule, we have conducted further investigation into the impact on the calculated LDOS of the FeTPP anion when an additional charge is initially positioned on the Fe atom (see Figs S2 and S3 for details). Our investigations reveal that in its neutral state, the electronic structure of the FeTPP-L molecule exhibits a high-spin configuration (s = 1) similar to octahedral complexes, resulting in a geometrical arrangement for which the surrounding pyrroles groups of the molecule are alternately slightly tilted up and down. In this arrangement, the central iron atom carries a slight positive charge (~ - 0.653 $\bar{e}$, Fig. S2), consistent with previous observations (Fig. 7b), with the most significant disparity between spin-up and spin-down evident in the Fe:$3d_{xz}$ and Fe:$3d_{yz}$ orbitals. Upon adding 0.5 electrons to the Fe atom, the subsequent stationary Bader charge analysis, after relaxation, indicates that the Fe atom also assumes a cationic state, having lost 0.683 electronic charges. A comprehensive analysis

reveals that the most notable Bader charge variation between the neutral state and the charged state predominantly impacts the spin-down component of the Fe:$3d_{x^2-y^2}$ and Fe:$3d_{z^2}$ orbitals in the negatively charged FeTPP molecule. The total charge (sum of spin-up and spin-down charges) at the Fe atom of the neutral FeTPP molecule is 6.71 electrons, while it amounts to 7.04 electrons for the negatively charged molecule. Consequently, the difference in total charge at the Fe atom, i.e., 0.33 electrons, suggests that the Fe atom retains 66 % of its additional charge at the Fe atom after relaxation. Hence our calculation method indicates that 34 % of the added electronic charge is delocalized over the FeTPP molecule.

The localization/delocalization effect is further established when comparing the calculated LDOS images of both a neutral FeTPP-L molecule and an anion FeTPP-L molecule as considered above (Fig. S4). The subsequent calculation of LDOS difference (neutral – charged) reveals partial relocalization of LDOS values around the central Fe atom, as well as in the vicinity of the upper left and lower right phenyl rings, attributable to the additional charge. This relocalization significantly differs from what is observed in Fig. 7d and indicates that specific conditions are necessary for the additional charge to become further delocalized within the surrounding macrocycle pyrroles, if it is initially injected at the Fe atom during the subsequent electronic loading process. Indeed, delocalization of the additional charge can be facilitated by specific vibrational modes of the iron atom that are coupled to the tunnel current flux, potentially resulting in a very efficient charge transfer from the iron atom to the porphyrin macrocycle[59]. This process is known to be favored when inelastic tunneling electrons lose some of their energy, enabling them to couple with the vibrational modes of the adsorbate. Such coupling facilitates a charge transfer from the iron atom to the porphyrin macrocycle, potentially enabling the loading of multiple electronic charges into a single molecule.

In this context, two important parameters may also influence the probability of a neutral FeTPP-L(R) molecule accepting one or multiple additional electronic charges in its structure and delocalizing them: (i) the orientation of the Fe atom relative to the molecular plane of the porphyrin macrocycle, and (ii) the initial spin state of the Fe atom within the porphyrin. To investigate these aspects, we computed the Bader charge variation for each atom of a FeTPP molecule relaxed in the gas phase (i.e., having a flat structure, as depicted in Fig. S5) under three different initial spin states: s = 2, 1, and 0, both before

and after receiving an additional 0.6 ē at the Fe atom. Note that in this case, we intentionally loaded the Fe atom with 0.6 ē to slightly enhance the delocalization process.

These calculations, presented in Fig. S5, show firstly, that the final charge state of the Fe atom is markedly more impacted by its initial spin state s = 2 compared to the other spin states s = 1 or s = 0. A quick comparison between Fig. S5b and Fig. 7b (s = 1) reveals that the Fe atom is slightly less cationic when the FeTPP molecule is in a flat configuration (with a loss of 0.59 ē, Fig. S5b) compared to its octahedral conformation (with a loss of 0.653 ē, Fig. 7b), indicating that the electronic reorganization is more pronounced for the FeTPP with an octahedral conformation. Furthermore, a closer examination of the total charge variation ($\Delta Q_{tot.}$) at the Fe atom between the neutral and charged states indicates that $\Delta Q_{tot.}$ = 0.621 ē, 0.517 ē, and 0.510 ē for s = 2, 1, and 0, respectively. Considering that the added electronic charge worth 0.6 ē, the trends revealed by this calculation indicate that the added charge tends to remain localized at the injection point for higher spin values.

This is further emphasized by analyzing the differences in Bader charges (neutral minus charged) for each of the initial spin states considered in the FeTPP molecule (s = 2 to 0 in Figs. S5g to S5l). Particularly notable is the negative Bader charge difference, signifying the transfer of charge from the Fe atom to the porphyrin macrocycle, a phenomenon prominently observed for s = 1 and 0. In these figures (Figs. S5g to S5l), the Bader charge variation at the Fe atom is deliberately set to zero for clarity.

In this context, these investigations clearly indicate the possibility of loading additional electronic charges into the FeTPP-L(R) molecular conformations, with the potential for the charge injection point to be localized at a different site from where the additional electronic charge is stored and subsequently delocalized. Although we did not, for this study, investigate the formation of FeTPP anions by positioning the STM tip at various locations on the molecule, our results lay the groundwork for the future utilization of such molecular devices as nanoscale batteries or nanodevices aimed at energy transport. Note that the DFT calculation of the LDOS distribution for the FeTPP cation is not relevant here, as the experimental STM image of this configuration could not be observed in a stationary state. This prevents us from determining which spatial area of the molecule this type of charge state modification affects.

5. CONCLUSIONS

Our investigations unveil that the charge variations in FeTPP molecules anion can be experimentally elucidated by examining the spatial variations in brightness within the STM image. This serves as a signature of charge delocalization in the electronic stationary state of the molecular anion. Our theoretical investigations, combined with STM current hysteresis measurements and specific dI/dV signatures, indicate the potential to create, stabilize, and manipulate a molecular anion on the CaF_2/Si(100) surface before returning it to its neutral state. Density functional theory is utilized, employing specifically tailored mixed-valence electronic atomic structures, to simulate and illustrate the variation of the added electronic charge and its dispersion within the molecule. Our findings underline that the stabilization of the molecular FeTPP anion is related to a reorganization of the spin charge state leading to specific spatial distribution of the magnetic moment in the molecule, as evidenced by the experimental STM image difference. Therefore, our work indicates that the control of the initial spin state as well as the molecular structure is crucial to enable efficient charge loading in the FeTPP molecule. Our findings also suggest that charge storage in adsorbed FeTPP can be manipulated on semi-insulating layers such as the CaF_2/Si(100) surface, offering promising prospects for applications related to energy storage and nanoscale charge transfer devices.

ASSOCIATED CONTENT

Supporting information

The Supplementary information is available for this article at: xxx

Details of the statistical analysis of the excitation process, the calculated electronic structure of the Fe and N atoms of the FeTTP molecule in both its neutral and anionic states, computed LDOS of the neutral and anionic FeTPP molecule when adsorbed on the CaF2/Si(100) surface, along with their atomic charge distribution and the resulting LDOS difference, as well as Bader charge comparisons of a FeTPP molecule in the gas phase for three different spin states in both

its neutral and anionic states, details of dI/dV spectroscopy on the charged FeTPP, KS orbitals of the FeTPP in gas phase compared to the PDOS of the same molecule when adsorbed on the CaF_2/Si(100) surface and comparison with the cation and anion.

AUTHORS INFORMATION

Corresponding author:

Damien Riedel - Institut des Sciences Moléculaires d'Orsay(ISMO), CNRS, Univ. Paris Sud, Université Paris-Saclay, F-91405 Orsay, France. ORCID : 0000-0002-7656-5409,

Email: damien.riedel@universite-paris-saclay.fr

Web site: mnd-sciences.com

Authors

Eric Duverger, Institut FEMTO-ST, Univ. Bourgogne Franche-Comté, CNRS, F-25030 Besançon, France, ORCID : 0000-0002-7777-8561

Notes

The authors declare no competing financial interests.

ACKNOWLEDGEMENTS

This work is supported by the ANR through the CHACRA project (ANR-18-CE30-0001). DR would like to thank *the federation lumière matière* (LUMAT) for the access to the MESOLUM calculation cluster. E.D. wishes to thank *the Mesocentre de calcul* of the Franche-comté University and the Communauté d'Agglomeration du Pays de Montbeliard (convention PMA-UFC). All the authors discussed the results and contributed to the manuscript writing. D.R. supervised the project.

FIGURES CAPTIONS

Figure 1: (a) and (b) 43.9 x 43.9 Å occupied state STM topographies (V_s = -2.4 V, I = 10 pA) of the two adsorption conformations of the FeTPP in the left (a) and right (b) orientations (i.e. noted FeTPP-L and FeTPP-R, respectively). (c) and (d) ball-and-stick representation (top view) of the adsorption configurations of FeTTP-L and FeTPP-R physisorbed on the CaF_2/Si(100) surface. (e) and (g), (g) and (h) ball-and-stick representation (side view) of the adsorption configuration of FeTTP-L and FeTPP-R, respectively.

Figure 2: (a) to (f) 36.3 x 36.3 $Å^2$ occupied state STM topographies (V_s = -2.4 V, I = 7 pA) series of FeTPP molecule, initially in the FeTPP-L conformation, following several types of excitations (red circle). The light brown arrows between the panels indicate the order of the manipulation steps (see also the numbers on the lower left corner of each panel). A voltage pulse in (a) ($V_{exc.}$ = + 2.5V, 6 - 10 s) is applied at the center of the molecule. (b) Subsequent occupied state STM topography (V_s = -2.4 V, I = 7 pA) of the same area. (d) Occupied state STM topography (V_s = -2.4 V, I = 7 pA) of the same area as in (b) showing that the FeTPP molecular conformation is back as in (a). (c) Occupied state STM topography (V_s = -2.4 V, I = 7 pA) of the same area, following the excitation (V_s = + 2.5V, 6 - 10 s) applied in (d). (e) STM topography (V_s = -2.4 V, I = 7 pA) of the same area following the excitation (V_s = - 2.4V, 6 - 10 s) applied in (c). (f) STM topography (V_s = -2.4 V, I = 7 pA) of the same area, following an excitation (V_s = - 2.4V, 6 - 10 s) applied in (d). (g) ball-and-stick representation of the first layers of the surface on which is adsorbed the FeTPP molecule as in (c). (h) LDOS of the FeTPP molecule as described in (g).

Figure 3: dI/dV curves showing the hysteresis behavior recorded from a neutral FeTPP molecule (① → ②, black curve) switching to its ionic state (③ → ④, red curve).

Figure 4: (a) 35.1 x 35.1 Å occupied state STM topographies (V_s = -2.4 V, I = 7 pA) of a FeTPP-L molecule adsorbed on CaF_2/Si surface. The blue, green and red circles stand for the phenyls, pyrroles and surface positions, respectively, at which the dI/dV curves are acquired in (b). (b) Series of dI/dV curves acquired on the FeTPP molecule as indicated in (a). The colors of the dI/dV curves match the colors of the circles in (a). (c) dI/dV curve acquired on the FeTPP molecule in its intermediate straddle configuration acquired at several positions (red circles) as indicated in the inset picture.

Figure 5: (a) and (b) 22.3 x 22.3 Å occupied state STM topographies (V_s = -2.4 V, I = 7 pA) of the FeTPP-L and FeTPP-G molecules on the CaF_2/Si surface. (c) and (d) 22.3 x 22.3 Å occupied state STM topographies (V_s = -2.4 V, I = 7 pA) of the FeTPP-L and FeTPP-G in its ionic state. (e) and (f) represent the calculated difference of the STM topographies resulting from (a) minus (b) and (b) minus (d), respectively.

Figure 6: (a) Kohn-Sham orbital energies of a neutral FeTPP-GP in gas phase with examples of spatial charge density distribution. The corresponding molecular structure is depicted in the right lower corner of the figure. The frontiers Kohn-Sham orbitals (-1.9 eV and -6.2 eV) are mostly located at the porphyrin macrocycle whereas several groups of Kohn-Sham orbitals compose the occupied and unoccupied states of the four phenyl groups around the molecule (-8.5 eV and 0.9 eV). (b) Comparison of the calculated Kohn-Sham orbital relative energies for a neutral FeTPP molecule (depicted by black and red circles), a cation (indicated by blue labels), and an anion (identified with green labels) in the gas phase. The energy values of the occupied Kohn-Sham orbitals of the phenyl groups of each species are shifted to fit the one observed experimentally in the dI/dV curves at -2.8 eV for the neutral FeTPP molecule and at -3.2 eV for the negative and positive FeTPP molecules. The on-scale profiles of the experimental dI/dV curves shown in Fig. 4 are recalled in Fig. S8. Colored vertical arrows indicate the latest filled Kohn-Sham orbital for each species.

Figure 7: (a) Calculated LDOS image (isodensity = 4.24 x 10^{-8} ē.$Å^{-1}$) of the neutral FeTPP-G adsorbed on the CaF_2/Si(100)surface. (b) Bader charge analysis of the neutral FeTPP-L (without representing the

surface, s = 1) as compared to the initial valence charge state as described in the methods section with Fe: $4s^2$ $3d^6$, C:$2s^2$ $2p^2$, N:$2s^2 2p^3$, H:$1s^1$. The lateral color scale in (b) indicates a maximum of charge variation (red) at 0.253 ē and a minimum of -0.653 ē (blue) mainly located at the nitrogen and iron atoms, respectively. (c) Calculated LDOS image (isodensity = 4.24 x 10^{-8} ē.$Å^{-1}$) of the negatively charged FeTPP-G adsorbed on the CaF_2/Si(100) surface. (d) Calculated LDOS image difference made from panel (a) minus (c). The inset in (d) is recalled from Fig. 5e for comparison. (e) and (f) Calculated Bader spin up and spin-down atomic charge state representation of the FeTPP-L (without representing the surface), respectively. (g) and (h) Calculated magnetic moment of the FeTPP-L as the difference of the $Q_{spin\text{-}up}$ minus $Q_{spin\text{-}down}$ charge difference for the positive and negative scales, respectively.

REFERENCES

[1]Wahadoszamen, MD.; Margalit, I.; Ara, A.M.; van Grondelle, R.; Noy, D. The role of charge-transfer states in energy transfer and dissipation within natural and artificial bacteriochlorophyll proteins. *Nature Comm.* **2014**, 5, 5287.

[2]Steurer, W.; J. Repp, J.; Gross, L.; Scivetti, I.; Persson, M.; Meyer, G. Manipulation of charge state Au atoms on Insulating Multilayer films. *Phys. Rev. Lett.* **2015**, 114, 036801.

[3]Mülleggera, S.; Rashidia, M.; Schöfbergerc, W.; Kocha, R. Single-molecule chemical reduction induced by low-temperature scanning tunneling microcopy: a case study of Gold-prphyrin on Au(111). *Surf. Sci.* **2018**, 678, 157-162.

[4]Miwa, K.; Imada, H.; Kawahara, S.; Kim, Y. Effects of molecule-insulator interaction on geometric property of a single phthalocyanine molecule adsorbed on an ultrathin NaCl film. *Phys Rev. B* **2016**, 93,165419.

[5]Scheuerer, P.; Patera, L.L.; Simbürger, F.; Queck, F.; Swart, I; Schuler, B.; Gross, L.; Moll, N.; Repp. J. Charge induced Structural Changes in a Single Molecule Investigated bu Atomic force Microscope, *Phys. Rev. Lett.* **2019**, 123, 066001.

[6]Yu, P.; Kocić, N.; Repp, J.; Siegert, B.; Donarini, A. Apparent Reversal of Molecular Orbitals Reveals Entanglement, *Phys. Rev. Lett.* **2017**, 119, 056801.

[7]Jaculbia, R.B.; Imada, H.; Miwa, K.; Iwasa, T.; Takenaka, M.; Yang, B.; Kazuma, E.; Hayazawa, N.; Taketsugu, T.; Yousoo, K. Single-molecule resonance Raman effect in a plasmonic nanocavity, *Nat. Nano.* **2020**, 15, 105-110.

[8]Pörtner, M.; Wei, Y.; Riss, A.; Seufert, K.; Garnica, M.; Barth, J.V.; Seitsonen, A.P.; Diekhöner, L.; Auwärter, W. Charge State Control of $F_{16}CoPc$ on h-BN/Cu(111). *Adv. Mat. Inter.* **2020**, 7, 2000080.

[9]Swart, I.; Sonnleitner, T.; Niedenführ, J.; Repp, J. Controlled lateral manipulation of molecule on Insulating Films by STM. *Nano Lett.* **2012**, 12, 1070-1074.

[10]Yan, S.; Ding, Z.; Xie, N.; Gong, H.; Sun, Q.; Guo, Y.; Shan, X.; Meng, S.; Lu, X. Turning on and off the Rotational Oscillation of a single Molecular Charge State, *ACS Nano* **2012**, 6, 4132-4136.

[11]Bellec, A.; Chaput, L.; Dujardin, G.; Riedel, D; Stauffer, L.; Sonnet, Ph. Reversible charge storage in a single silicon atom. *Phys. Rev. B* **2013**, 88, 241406.

[12]Patera, L.L.; Queck, F.; Repp, J. Imaging Charge localization in a conjugated oligophenylene, *Phys. Rev. Lett.* **2000**, 125, 176803.

[13]Patera, L.L.; Queck, F.; Scheuerer, P.; Moll, N.; Repp, J. Accessing a Charged Intermediate State Involved in the Excitation of Single Molecules, *Phys. Rev. Lett.* **2019**, 123, 016001.

[14]Ryndyk, D.A.; D'Amico, P.; Cuniberti, G.; Richter, K. Charge memory polaron effect in molecular junctions, *Phys. Rev. B* **2008**, 78, 085409.

[15]Wu, S.W.; Ogawa, N.; Nazin, G.V.; Ho, W. Conductance hysteresis and switching in a Single-Molecule Junction, *J. Of Phys. Chem. C* **2008**, 5241-5244.

[16]Kaiser, K.; Lieske, L.A.; Repp. J.; Gross, L. Charge-state lifetimes of single molecules on ultrathin insulating films. *Nat. Comm.* **2023**, 14, 4988.

[17]Ham, U.; Ho, W. Spin Splitting Unconstrained by Electron Pairing: The Spin-Vibronic States. *Phys. Rev. Lett.* **2012**, 108, 106803.

[18]Mohn, F.; Gross, L.; Moll, N.; Meyer, G. Imaging the charge distribution within a single molecule. *Nat. Nano.* **2012**, 7, 227-231.

[19]Yengui, M.; Pinto, H.P.; Leszczynski, J.; Riedel, D. Atomic scale study of corrugating and anticorrugating states on the bare Si(100) surface. *J. Phys. Condens. Mat.* **2015**, 27, 045001.

[20]Bellec, A.; Ample, F.; Riedel, D.; Dujardin, G.; Joachim, Ch. Imaging molecular orbitals by scanning tunneling microscopy on a passivated semiconductor. *Nano Lett.* **2008**, 9, 144–147.

[21]Bellec, A.; Riedel, D.; Dujardin, G.; Boudria, O.; Chaput, L.; Stauffer, L.; Sonnet, Ph. Nonlocal activation of a bistable atom through a surface state charge-transfer process on Si(100)-(2×1):H. *Phys. Rev. Lett.* **2010**, 105, 048302.

[22]Schofield, S. R.; Studer, P.; Hirjibehedin, C.F.; Curson, N.J.; Aeppli, G.; Bowler, D.R. Quantum engineering at the silicon surface using dangling bonds. *Nat. Commun.* **2013**, 4, 1649.

[23]Yengui, M.; Duverger, E.; Sonnet, P.; Riedel, D. A two-dimensional ON/OFF switching device based on anisotropic interactions of atomic quantum dots on Si(100):H. *Nat. Commun.* **2018**, 8 2211.

[24]Duverger, E.; Boyer, A.G.; Sauriat-Dorizon, H.; Sonnet, P.; Stephan, R.; Hanf, M.C.; Riedel, D. Two-dimensional functionalized ultrathin semi-insulating CaF_2 layer on the Si(100) surface at a low temperature for molecular electronic decoupling, *ACS Appl. Mater. Interfaces* **2020**, 12, 29661–29670.

[25]Wang, Y. ; Boyer, A.G.; Sauriat-Dorizon, H.; Duverger, E.; Riedel, D. Electronic Structure and Bistable Conformational Study of the Tetraphenylporphyrin Erbium(III) Acetylacetonate Complex on the CaF_2/Si(100) Surface at Low Temperatures. *J. Phys. Chem. C* **2021**, 125, 14453-14460.

[26]Duverger, D.; Riedel, D. Periodically spaced CaF_2 semi-insulating thin ribbons growth study on the Si(100) surface. *Mater. Adv.* **2022**, 3, 8241.

[27]Auwärter, W.; Écija, D.; Klappenberger, F.; Barth, J.V. Porphyrins at interfaces. *Nat. Chem.* **2015**, 7, 105-120.

[28] Miller, D.P.; Hooper, O.J.; Simpson, S.; Costa, P.S.; Ymińska, N.; McDonnel, S.M.; Bennett, J.A.; Enders, A.; Zurek, E. Electronic Structure of Iron Porphyrin Adsorbed to the Pt(111) Surface. *J. Phys. Chem. C* **2016**, 120, 29173–29181.

[29]Ramos, P.; Mankarious, M.; Pavanello, M.; Riedel, D. Probing charge transfer dynamics in a single iron tetraphenylporphyrin dyad adsorbed on an insulating surface. *Nanoscale* **2018**, 10, 17603.

[30]Sorgues, S.; Poisson; P.; Raffael, K.; Krim, L.; Soep, B.; Shafizadeh, N. Femtosecond electronic relaxation of excited metalloporphyrins in the gas phase. *J. Chem. Phys.* **2006** 124, 114302.

[31]Tang, H.; Tarrat, N.; Langlais, V.; Wang, Y.; Adsorption of iron tetraphenylporphyrin on (111) surfaces of coinage metals: a density functional theory study. *Beilstein J. Nanotechnol.* **2017**, 8, 2484–2491.

[32]Bouatou, M.; Harsh, R.; Joucken, F.; Chacon, C.; Repain, V.; Bellec, A. Girard, Y.; Rousset, S.; Sporken, R.; Gao, F.; Brandbyge, M.; Dappe, Y.J.; Barreteau, C.; Smogunov, A.; Lagoute, J. Intraconfigurational Transition due to Surface-Induced Symmetry Breaking in Noncovalently Bonded Molecules. *J. Phys. Chem. Lett.* **2020**, 11, 9329–9335.

[33]Römelt, C.; Song, J.; Tarrago, M.; Rees, J.; van Gastel, M.; Weyhermüller, T.; DeBeer, S.; Bill, E.; Neese, F.; Ye, S.; Electronic Structure of a Formal Iron(0) Porphyrin Complex Relevant to CO_2 Reduction. *Inorg. Chem.* **2017**, 56, 4745–4750.

[34]Sedona, F.; Marino, M.D.; Forrer, D.; Vittadini, A.; Casarin, M.; Cossaro, A.; Floreano, L.; Verdini, A.; Sambi, M. Tuning the catalytic activity of Ag(110)-supported Fe phthalocyanine in the oxygen reduction reaction. *Nat. Mat.* **2012**, 11, 970-977.

[35]Aziz, M.S. Electrical properties of Π-conjugated Fe-TPP molecular solar cell device. *Solid-State Electronics* **2008**, 52, 1145-1148.

[36]El-Nahass, M.M.; Metwally, H.S.; El-Sayed, H.E.A.; Hassanien, A.M. Electrical and photovoltaic properties of FeTPPCl/p-Si heterojunction. *Synthetic Metals*, **2011**, 161, 2253-2258.

[37]Chiaravalloti, F.; Dujardin, G.; Riedel, D.; Pinto, H.P.; Foster, A.S. Atomic-scale study of the adsorption of calcium fluoride on Si(100) at low-coverage regime. *Phys. Rev. B* **2011**, 84, 155433.

[38] Gaussian 09, Revision A.02, Frisch, M. J. et al. Gaussian, Inc., Wallingford CT, 2016.

[39]Soler, J.M.; Artacho, E.; Gale, J.D.; García, A.; Junquera, J.; Ordejón, P.; Sanchez-Portal, P. The SIESTA Method for Ab Initio Order-N Materials Simulation. *J. Phys. Chem. C* **2002**, 14, 2745-2779.

[40]Ordejón, P.; Artacho, E.; Soler, J. M. Self-Consistent Order-N Density-Functional Calculations for Very Large Systems. *J. Phys. Chem. C* **1996**, 53, 10441-10444.

[41]Hohenberg, P.; Kohn, W. Inhomogeneous Electron Gas. *J. Phys. Chem. C* **1964**, 136, 864-871.

[42]Kohn, W.; Sham, L. J. Self-Consistent Equations Including Exchange and Correlation Effects. *J. Phys. Chem. C* **1965**, 140, 1133-1138.

[43]Dion, M.; Rydberg, H.; Schröder, E.; Langreth, D. C.; Lundqvist, B. I. Van der Waals Density Functional for General Geometries. *J. Phys. Chem. C* **2004**, 92, 246401.

[44]Perdew, J. P.; Burke, K.; Ernzerhof, M. Generalized Gradient Approximation Made Simple. *J. Phys. Chem. C* **1996**, 77, 3865-3868.4

[45]Román-Pérez, G.; Soler, J. M. Efficient Implementation of a Van der Waals Density Functional: Application to Double-Wall Carbon Nanotubes. *J. Phys. Chem. C* **2009**, 103, 096102.

[46]Poloni, R.; Iniguez, J.; Garcia, A.; Canadell, E. An Efficient Computational Method for Use in Structural Studies of Crystals with Substitutional Disorder. *J. Phys. Chem. C* **2010**, 22, 415401.

[47]Bader, R. F. W. A Quantum Theory of Molecular Structure and Its Applications. *J. Phys. Chem. C* **1991**, 91, 893-928.

[48]Henkelman, G.; Arnaldsson, A.; & Jónsson, H. A fast and robust algorithm for Bader decomposition of charge density. *Computational Materials Science*, **2006**, 36, 354-360.

[49]Sanville, E.; Kenny, S. D.; Smith, R.; & Henkelman, G. Improved grid based algorithm for Bader charge allocation. *Journal of Computational Chemistry*, **2007**, 28, 899-908.

[50] See SIEASTA manual page 108 at https://siesta-project.org/SIESTA_MATERIAL/Docs/Manuals/siesta-4.1.5.pdf

[51]Ramos, P. Mankarious, M.; Pavanello, M. Riedel, D. Probing charge transfer dynamics in a single iron tetraphenylporphyrin dyad adsorbed on an insulating surface. *Nanoscale* **2018**, 10, 17603.

[52]Riedel, D.; Single molecule manipulation at low temperature and laser scanning tunnelling photo-induced processes analysis through time-resolved studies. *J. Phys.:Condens. Matter* **2010**, 22, 264009.

[53]Mayne, A.J.; Dujardin, G.; Comtet, G.; Riedel. D.; Electronic Control of Single-Molecule Dynamics. *Chem. Rev.* **2006**, 106, 4355−4378.

[54]Riedel, R.; Bocquet, M.L.; Lesnard, H. ; Lastapis, M. Lorente, N. ; Sonnet, P. Selective scanning tunnelling microscope electron-induced reactions of single biphenyl molecules on a Si(100) surface. *JACS* **2009**, 131, 7344-7352.

[55]Labidi, H.; Sonnet, Ph.; Riedel, D. Electronic Control of the Tip-Induced Hopping of an Hexaphenyl-Benzene Molecule Physisorbed on a Bare Si (100) Surface at 9 K, *J. Phys. Chem. C* **2013**, 117, 13663–13675.

[56]Steurer, W.; Repp, J.; Gross, L.; Scivetti, I.; Persson, M.; Meyer, G. Manipulation of the Charge State of Single Au Atoms on Insulating Multilayer Films. *Phys. Rev. Lett.* **2015**, 114, 036801.

[57]Gross, L.; Mohn, F.; Liljeroth, P.; Repp, J.; Giessibl, F.J.; Meyer, G.; Measuring the Charge State of an Adatom with Noncontact Atomic Force Microscopy. *Science*, **2009**, 324, 1428-1431.

[58]Tu, X. W.; Mikaelian, G., Ho, W. Controlling Single-Molecule Negative Differential Resistance in a Double-Barrier Tunnel Junction. *Phys. Rev. Lett.* **2008**, 100, 126807.

[59]Berthe, M.; Urbieta, A.; Perdigaõ, L.; Grandidier, B.; Deresmes, D.; Delerue, C.; Stiévenard, D.; Rurali, R.; Lorente, N.; Magaud, L. et al. Electron Transport via Local Polarons at Interface. Atoms. *Phys. Rev. Lett.* **2006**, 97, 206801.